International Journal of Mathematical Archive-8(7), 2017, 48-64
Available online through www.ijma.info ISSN 2229 – 5046

AN EXACT ANALYSIS ON FREE CONVECTIVE HEAT AND MASS TRANSFER FLOW OF MICROPOLAR FLUID IN POROUS MEDIA WITH FLUCTUATING WALL EMPERATURE

[1]SANJIB SENGUPTA*, [2]RESHMI DEB

[1,2]Department of Mathematics, Assam University, Silchar, Assam, India.

(Received On: 14-06-17; Revised & Accepted On: 05-07-17)

ABSTRACT

In this paper an exact analysis is made to study the free convection mass transfer flow of a micropolar fluid past a vertical porous plate embedded in Darcian porous media. The semi- infinite plate is subjected to a constant suction velocity and the temperature near the plate is supposed to get jumped exponentially. The governing system of partial differential equations is first transformed into a system of ordinary differential equations using a set of asymptotic transformations. A parametric study demonstrating the physical influence of the micro-gyration parameter, vortex viscosity parameter, dimensionless material parameter and proportionality parameter on the fluid velocity, microrotation velocity, coefficients of shear stress and couple stresses as well as Nusselt and Sherwood numbers is performed. The closed form of solutions obtained is finally validated through graphs and in tabular form and the physical aspects of the problem are highlighted and discussed theoretically. The results show that, the linear velocity initially decreases thereafter increases due to increase in vortex viscosity parameter, while for an increase in vortex viscosity parameter, an increasing trend is observed for angular velocity. The increase in values of Prandtl number decreases the skin-friction co-efficient, while it is found increasing the couple stress coefficient. A comparative study reveals that, the coefficients of skin-friction as well the couple stresses are less in micropolar fluids than in conventional Newtonian fluids.

Keywords: *Free Convection, mass transfer, micropolar fluid, porous media and fluctuating wall temperature.*

MSC 2010 classification: *76A05, 76S05, 80A20.*

Nomenclature

$\overline{C}$	Species concentration
$\overline{C}_m$	Species concentration at the plate
C_p	Specific heat at constant pressure
$\overline{C}_\infty$	Species concentration in the free stream
D_M	Coefficient of mass diffusion
$\vec{g}$	Acceleration due to gravity
G_M	Thermal Grashof number
G_r	Solutal Grashof number
K	Thermal conductivity
Nu_R	Nusselt number (real part)
Pr	Prandtl number
Sc	Schmidt number
Sh_R	Sherwood number (real part)
Sr	Soret number
t	Time variable(non-dimensional)
$\bar{t}$	Time variable (dimensional)
$\overline{T}$	Fluid temperature

Corresponding Author: [1]Sanjib Sengupta, [2]Reshmi Deb*
[1,2]Department of Mathematics, Assam University, Silchar, Assam, India.

$\overline{T}_m$	Temperature at the plate
$\overline{T}_\infty$	Temperature in the free stream
u	First component of fluid velocity (non-dimensional)
$\overline{u}$	First component of fluid velocity (dimensional)
u_o	Mean plate velocity (non-dimensional)
u_R	Real part of u
y	y-co-ordinate (non-dimensional)
$\overline{y}$	y- co-ordinate (dimensional)
v	Second component of fluid velocity
V_O	Mean suction velocity
$\overline{v}$	Second component of fluid velocity (dimensional)
j	Vortex viscosity parameter

Greek Symbols

θ	Non-dimensional temperature
ρ	Fluid density
ϕ	Non-dimensional species concentration
ω	Frequency of oscillation
η	spin gradient viscosity
ν	Kinematic viscosity
ν_r	Vortex viscosity
θ_R	Real part of θ
ϕ_R	Real part of ϕ

Subscripts

m	Conditions on the wall
∞	Free stream conditions

1. INTRODUCTION

The theory of natural convection heat and mass transfer effects in non-Newtonian fluid flow is becoming well motivated area of research work due to its diverse applications in various fields such as geothermal engineering, nuclear reactor, petroleum industries, chemical process industries, liquid metals and plasma flows, chemical catalytic reactor, thermal insulation, energy conservation and underground disposal of nuclear waste materials and many more. Natural or free convection occurs when the fluid flow appears as a consequence of the heat-transfer phenomena due to buoyancy forces caused by density differences affected by temperature gradients in an external force field. Natural convection takes place in all heat convection problems under gravity. The phenomenon of mass fluxes caused due to concentration gradients is known as the mass transfer. The free convective heat and mass transfer boundary layer flow generated in a fluid adjacent to a heated, vertical infinite / semi-infinite plate is one of the basic flows in heat and mass transfer phenomena research. Alam *et al.* [1] studied an unsteady two dimensional forced convection flow of a micropolar fluid along a wedge. Ali *et al.* [2] investigated the effects of non-Darcian and thermal dispersion of laminar free convection boundary layer flow of a micropolar fluid in porous medium. A number of studies on the laminar free convection heat and mass transfer flow of Newtonian as well as non-Newtonian fluids have been found in literature, these do not give satisfactory results if the fluid is a mixture of heterogeneous means such as liquid crystals, ferro-liquid, liquid with polymer additives, which is more realistic and important from technological point of view. The basic concept of micropolar fluids have governed from the necessity to model many engineering processes involving non-Newtonian fluids containing micro constituents such as colloidal fluids, blood flow, lubricants and suspension fluids that cannot be described by the theory of Newtonian fluids. Several researchers have attracted by micropolar fluids because of the equation governing the flow of micropolar fluid that involves a microrotation vector and a gyration parameter in addition to the definitive velocity vector field. These parameters play a major role in engineering and allied areas. Micropolar fluid is a subject of microphoric fluid theory. A comprehensive review of the subject and applications of micropolar fluid mechanics was given by Arimanet *et. al.* [3, 4]. Ahmad and Hussain[5] considered recently theconvective heat transfer for MHD micropolar fluids flow through porous medium over a stretching surface. Bakr [6] considered the steady and unsteady MHD micropolar mass transfers flow with constant heat source in a rotating frame of reference, taking an oscillatory plate velocity and a constant suction velocity. Bejan[7] investigated

the free convective heat and mass transfer flows through an infinite / semi – infinite plate. Chaudhury *et al.* [8] obtained perturbed form of solutions for unsteady magnetopolar free convection flow in a porous medium with radiation and variable suction in a slip flow regime. It is observed that, the unsteady heat and mass transfer of fluid flowand transport phenomena in the porous media are important processes in many engineering applications, e.g., heat exchanger, pack-sphere bed, electronic cooling, chemical catalytic reactors, heat pipe technology, etc. This type of unsteady flow model might find applications in the study of corrosion effects of porous sediments under polar fluid flow. In the case of polar fluid flow through porous sediment, the inclusion of rotational viscosity in the Darcy term is an imperative due to the small, pore-level length scales associated with this type of flow domain. Considering the significance of the aforesaid study, Cortell[9] investigated the **f**low and heat transfer of a fluid through a porous medium over a stretching surface with internal heat generation/absorption and suction/blowing. The unsteady natural convection heat transfer of a micropolar fluid over a vertical surface with constant heat flux was studied by Damseh *et al.* [10]. Das [11] analyzed the effect of first order chemical reaction and thermal radiation on MHD free convection heat and mass transfer flow of a micropolar fluid via a porous medium bounded by a semi-infinite porous plate with constant heat source in a rotating frame of reference. The theory of micropolar fluid developed by Eringen [12, 13] describes fluids by taking into account the microscopic effects arising from the local structure and microrotations of the fluid elements. After that, the micropolar fluid behaviors on steady MHD free convection mass transfer flow were investigated by Haque [14]. A significant amount of research work concerning micropolar fluid flow and effect of heat and mass transfer under different boundary conditions and in the presence of various physical effects has been reported. Javaherdeh et al. [15] recently obtained numerical solution for natural convection heat and mass transfer flow past a moving vertical plate with variable surface temperature and concentration in a porous medium in presence of a magnetic field.Kim [16,17] studied heat and mass transfer phenomena in micropolar flow over a vertical moving porous plate. Makinde [18] examined the transient free convection interaction with thermal radiation of an absorbing emitting fluid moving along a vertical permeable plate. Mohammad *et al.* [19] studied mixed convection boundary-layer flow of a micropolar fluid towards a heated shrinking sheet by homotopy analysis method. Oahimire and Olajuwon [20] studied the effects of radiation absorption and thermo-diffusion on MHD heat and mass transfer flow of a micro-polar fluid in the presence of the heat source. Very recently, Ojjela and Naresh [21] investigated the first-order chemical reaction and Soret and Dufour effects on an incompressible MHD combined free and forced convection heat and mass transfer of a micropolar fluid through a porous medium between two parallel plates. Prathap *et al.* [22] analyzed Fully-developed free-convective flow of micropolar and viscous fluids in a vertical channel. Raptis [23] investigated the free convective heat and mass transfer flows through an infinite / semi – infinite plate. Rashidi *et al.* [24] studied buoyancy effects in free convective heat and mass transfer flow over a permeable vertical stretching sheet in the presence of a magnetic field and thermal radiation. Rawat et al. [25] studied steady, fully developed MHD free convection heat and mass transfer of a micropolar fluid with heat generation or absorption. Seddek *et al.* [26] obtained analytical solution on flow of magneto micropolar fluid past a continuously moving plate with suction and blowing in presence of radiation. Soundalgekar [27] investigated the free convective heat and mass transfer flows through an infinite / semi – infinite plate. Yucel[28] considered the case of mixed convection micropolar fluid flow over horizontal plate with surface mass transfer.

In view of the above discussion and considering the constantly growing importance of the theory of micropolar fluids and its related properties, the objective of the present paper is to consider the free convective heat and mass transfer flow of micropolar fluids past a porous plate embedded in Darcian resistance media with fluctuating plate temperature. The methodology used to solve the present problem is the normal mode method and to the best of our knowledge a very few works is reported by this method to the theory of micropolar fluid as it can be used for the development of many complex situations in the theory of micropolar fluids. The models developed in this paper might find its applications in the study of lubrication problems in configurations possessing porous linings.

2. BASIC EQUATIONS AND ASSUMPTIONS TAKEN

2.1 Basic equations used:

The basic equations used to model the physical situation are as follows:

$$\overrightarrow{\nabla}.\vec{q} = 0 \qquad \text{(Continuity equation)}$$

$$\left[\frac{\partial}{\partial t}+\left(\vec{q}.\overrightarrow{\nabla}\right)\right]\vec{\mathrm{q}} = -\frac{1}{\rho}\overrightarrow{\nabla}p+\vec{g}+\left(\nu+\nu_r\right)\overrightarrow{\nabla}.\vec{q}+2\nu_r\,\mathrm{curl}\,\vec{\Omega}-\frac{1}{\overline{\overline{K}}}\left(\nu+\nu_r\right)\vec{q}$$

(Linear momentum equation)

$$\rho\mathrm{I}\left[\frac{\partial}{\partial t}+\left(\vec{q}.\overrightarrow{\nabla}\right)\right]\vec{\Omega} = \eta\,\overrightarrow{\nabla}^2\vec{\Omega} \qquad \text{(Angular momentum equation)}$$

$$\rho\mathrm{C_p}\left[\frac{\partial}{\partial t}+\left(\vec{q}.\overrightarrow{\nabla}\right)\right]\mathrm{T} = k\,\overrightarrow{\nabla}^2\overline{T} \qquad \text{(Energy equation)}$$

$$\left[\frac{\partial}{\partial t}+\left(\vec{q}.\vec{\nabla}\right)\right]\mathrm{C}=D_M\vec{\nabla}^2\bar{C} \qquad \text{(Concentration equation)}$$

In this case, $\vec{q}=\left(\bar{u}\ ,\bar{\mathrm{v}}\ ,0\right)$, $\vec{\Omega}=\left(\bar{\omega}\ ,0,\ 0\right)$ and $\vec{\nabla}=\left(\frac{\partial}{\partial \mathrm{x}}\ ,\frac{\partial}{\partial \mathrm{y}},\ 0\right)$

2.2 Approximations and assumptions considered:

The present study is based on the following set of assumptions as**:**

1. The fluid flow is restricted to laminar region.
2. The Boussinesq approximations are used as such all the velocities are considered as much smaller than the speed of light.
3. No magnetic field is applied on the flow.
4. The fluid is considered as Newtonian (i.e. dynamic viscosity is not a function of rate of deformation) and incompressible (i.e., density is constant).
5. The dynamic viscosity (ν), vortex viscosity (ν_r), spin gradient viscosity (η) and thermal conductivity (k) are taken as constant throughout the discussion.
6. The plate temperature as well as concentrations is assumed to be more than their respective values in the ambient (free stream) region.

3. MATHEMATICAL FORMULATION OF THE PROBLEM

A two - dimensional unsteady flow of a micropolar fluid past a permeable semi-infinite vertical plate embedded in Darcian porous media is considered for study. The *x*-axis is taken along the length of the plate while *y* - axis is considered perpendicular to the plate along the fluid region. It is assuming that, except pressure all other fluid properties are considered to be independent of *x*-scale variation.

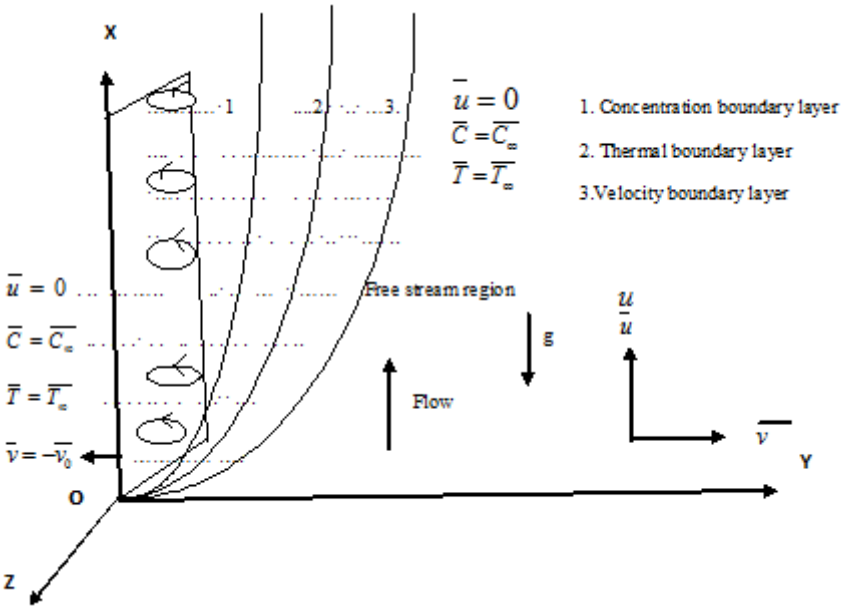

Figure 1: Schematic representation of flow configuration and co-ordinate system

The temperature and concentration of fluid particles are considered to be more than their free stream values. Using Boussinesque and boundary layer approximations a fluid model developed as:

Continuity Equation:

$$\frac{\partial \bar{v}}{\partial y}=0 \qquad (1)$$

Linear x-momentum equation

$$\frac{\partial \bar{u}}{\partial x}+\bar{v}\frac{\partial \bar{u}}{\partial y}=\left(\nu+\nu_r\right)\frac{\partial^2 \bar{u}}{\partial y^2}+2\nu_r\frac{\partial \bar{\omega}}{\partial y}+g\beta_T\left(\bar{T}-\bar{T_\infty}\right)+g\beta_C\left(\bar{C}-\bar{C_\infty}\right)-\frac{1}{K}\left(\nu+\nu_r\right)\bar{u} \qquad (2)$$

Angular momentum equation about x- axis

$$\left(\frac{\partial\bar{\omega}}{\partial\bar{t}}+\bar{v}\frac{\partial\bar{\omega}}{\partial\bar{y}}\right)\rho I=\eta\frac{\partial^2\bar{\omega}}{\partial\bar{y}^2} \tag{3}$$

Energy equation

$$\frac{\partial\bar{T}}{\partial\bar{t}}+\bar{v}\frac{\partial\bar{T}}{\partial\bar{y}}=\frac{k}{\rho C_p}\frac{\partial^2\bar{T}}{\partial\bar{y}^2} \tag{4}$$

Species continuity equation

$$\frac{\partial\bar{C}}{\partial\bar{t}}+\bar{v}\frac{\partial\bar{C}}{\partial\bar{y}}=D_M\frac{\partial^2\bar{C}}{\partial\bar{y}^2} \tag{5}$$

Subject to the boundary conditions as:

$$\bar{u}=0,\ \bar{v}=0,\ \bar{\omega}=0 \text{ for every } \bar{y}\le 0 \tag{6.1}$$

$$\bar{u}=0,\ \bar{v}=-V_0,(V_0>0),\ \bar{\omega}=-n\frac{\partial\bar{u}}{\partial\bar{y}},\bar{T}=\bar{T}_\infty+A\left(\bar{T}_m-\bar{T}_\infty\right)\exp\left(i\bar{\omega}t\right),\ \bar{C}=\bar{C}_m, \text{ for } \bar{y}=0 \text{ when t>0} \tag{6.2}$$

$$\bar{u}\to 0,\bar{\omega}\to 0,\bar{T}\to\bar{T}_{\infty,},\ \bar{C}\to\bar{C}_\infty \text{ for } \bar{y}\to\infty,t>0 \tag{6.3}$$

We introduce the following non-dimensional quantities as:

$$y=\frac{\bar{y}V_0}{\nu},\ u=\frac{\bar{u}}{V_0},\ v=\frac{\bar{v}}{V_0},\ t=\frac{V_0^{\,2}\bar{t}}{\nu},\ N=\frac{\nu\bar{\omega}}{V_0^{\,2}},\ \theta=\frac{\bar{T}-\bar{T}_\infty}{\bar{T}_m-\bar{T}_\infty},\ \phi=\frac{\bar{C}-\bar{C}_\infty}{\bar{C}_m-\bar{C}_\infty},\ K=\frac{\bar{K}V_0}{\nu^2},$$

$$G_r=\frac{g\beta_T\nu\left(\bar{T}_m-\bar{T}_\infty\right)}{V_0^{\,3}},\ G_m=\frac{g\beta_c\nu\left(\bar{C}_m-\bar{C}_\infty\right)}{V_0^{\,3}},\ j=\frac{\nu_r}{\nu},\ s=\frac{\rho\nu I}{n},\ P_r=\frac{\rho\nu C_p}{k},\ S_c=\frac{\nu}{D_M}$$

The non-dimensional form of equations is:

$$\frac{\partial u}{\partial t}-\frac{\partial u}{\partial y}=(1+j)\frac{\partial^2 u}{\partial y^2}+2j\frac{\partial N}{\partial y}+G_r\theta+G_m\phi-\frac{1+j}{K}u \tag{7}$$

$$\frac{\partial N}{\partial t}-\frac{\partial N}{\partial y}=\frac{1}{s}\frac{\partial^2 N}{\partial y^2} \tag{8}$$

$$\frac{\partial\theta}{\partial t}-\frac{\partial\theta}{\partial y}=\frac{1}{P_r}\frac{\partial^2\theta}{\partial y^2} \tag{9}$$

$$\frac{\partial\phi}{\partial t}-\frac{\partial\phi}{\partial y}=\frac{1}{S_c}\frac{\partial^2\phi}{\partial y^2} \tag{10}$$

With non-dimensional boundary conditions as

$$u(0,t)=0,v(0,t)=-1,\ N(0,t)=-n\frac{\partial u}{\partial y},\ \theta(0,t)=A\exp(i\omega t),\phi(0,t)=0,\ \forall\ t>0 \tag{11.1}$$

$$u(\infty,t)=0,\ N(\infty,t)=0,\ \theta(\infty,t)=0,\ \phi(\infty,t)=0,\ \forall\ t>0 \tag{11.2}$$

4. METHOD OF SOLUTION

To solve equations (7) to (10), we preferred to use a set of asymptotic series expansion forms as:

$$u(y,t)=\sum_{r_1=0}^{\infty}u_0(y)\frac{(i\omega t)^{r_1}}{r_1!},\ \theta(y,t)=\sum_{r_2=0}^{\infty}\theta_0(y)\frac{(i\omega t)^{r_2}}{r_2!},\ \phi(y,t)=\sum_{r_3=0}^{\infty}\phi_0(y)\frac{(i\omega t)^{r_3}}{r_3!}$$

$$N(y,t)=\sum_{r_4=0}^{\infty}N_0(y)\frac{(i\omega t)^{r_4}}{r_4!},$$

The equations (7), (8), (9) and (10) become,

$$(1+j)\frac{d^2u_0}{dy^2}+\frac{du_0}{dy}-\left(\frac{1+j}{K}+i\omega\right)u_0=-2j\frac{dN_0}{dy}-G_r\theta_0-G_m\phi_0 \tag{12}$$

$$\frac{d^2\theta_0}{dy^2}+P_r\frac{d\theta_0}{dy}-i\omega P_r\theta_0=0 \tag{13}$$

$$\frac{d^2\phi_0}{dy^2}+S_c\frac{d\phi_0}{dy}-i\omega S_c\phi_0=0 \tag{14}$$

$$\frac{d^2N_0}{dy^2}+s\frac{dN_0}{dy}-i\omega sN_0=0 \tag{15}$$

With the associated boundary conditions as:

$$u_0(0)=0, N_0(0)=-n\left(\frac{du_0}{dy}\right)_{y=0}, \theta_0(0)=A, \phi_0(o)=1 \tag{16.1}$$

$$u_0(\infty)=0, N_0(\infty)=0, \theta_0(\infty)=0, \phi_0(\infty)=0 \tag{16.2}$$

The solutions for linear velocity, angular velocity, temperature and concentrations are finally calculated as:

$$\begin{aligned} u_R(y) &= \left[e_1\cos(\omega t-\beta_4 y)-e_2\sin(\omega t-\beta_4 y)\right]\exp(-\alpha_4 y)\\ &+\left[b_1d_1\cos(\omega t-\beta_1 y)+b_1d_2\sin(\omega t-\beta_1 y)\right]\exp(-\alpha_1 y)\\ &-\left[b_2d_2\cos(\omega t-\beta_1 y)-b_2d_1\sin(\omega t-\beta_1 y)\right]\exp(-\alpha_1 y)\\ &+\left[d_3\cos(\omega t-\beta_2 y)+d_4\sin(\omega t-\beta_2 y)\right]\exp(-\alpha_2 y)\\ &+\left[d_5\cos(\omega t-\beta_2 y)-d_6\sin(\omega t-\beta_3 y)\right]\exp(-\alpha_3 y) \end{aligned}$$

$$\begin{aligned} N_R(y,t) &= \left[b_1\cos(\omega t-\beta_1 y)-b_2\sin(\omega t-\beta_1 y)\right]\exp(-\alpha_1 y)\\ &+\left[b_2\cos(\omega t-\beta_1 y)+b_1\sin(\omega t-\beta_1 y)\right]\exp(-\alpha_1 y) \end{aligned}$$

$$\theta_R(y,t)=A\exp(-\alpha_2 y)\cos(\omega t-\beta_2 y)$$

$$\phi_R(y,t)=\exp(-\alpha_3 y)\cos(\omega t-\beta_3 y)$$

Some quantities of engineering interest are discussed as follows:

(i) Skin-friction co-efficient at the plate:

The non – dimensional skin friction at the plate y=0 due to linear motion is calculated as:

$$\begin{aligned} \tau_w &= \left[(1+j)\frac{\partial u_R}{\partial y}+jN\right]_{y=0}\\ &= (1+j)\begin{bmatrix}(-\alpha_4e_1+e_2\beta_4-\alpha_1b_1d_1+b_1d_2\beta_1+\alpha_1b_2d_2+b_2d_1\beta_1-\alpha_2d_3+d_4\beta_2-d_5\alpha_3+d_6\beta_3)\cos\omega t\\ -(-\alpha_4e_2-e_1\beta_4-\alpha_1b_2d_1+b_2d_2\beta_1-\alpha_1b_1d_2-b_1d_1\beta_1-\alpha_2d_4-d_3\beta_2-d_6\alpha_3-d_5\beta_3)\sin\omega t\end{bmatrix}\\ &+j\left[(b_1\cos\omega t-b_2\sin\omega t)\right] \end{aligned}$$

The skin friction coefficient is obtained as:

$$C_f=\frac{2\tau_w}{V_0^{\,2}}=2(1+j(1-n))\left(\frac{\partial u}{\partial y}\right)_{y=0}$$

On further calculation we arrive at,

$$C_f = 2\left(1+ j(1-n)\right)\left[C_{f_1} \cos \omega t - C_{f_2} \sin \omega t \right]$$

Where, $C_{f_1} = -\alpha_4 e_1 + \beta_4 e_2 - \alpha_1 b_1 d_1 + \beta_1 b_1 d_2 + \alpha_1 b_2 d_2 + \beta_1 b_2 d_1 - \alpha_2 d_3 + \beta_2 d_4 - \alpha_3 d_5 + \beta_3 d_6$

$C_{f_2} = -\alpha_4 e_2 - \beta_4 e_1 - \alpha_1 b_2 d_1 + \beta_1 b_2 d_2 - \alpha_1 b_1 d_2 - \beta_1 b_1 d_1 - \alpha_2 d_4 - \beta_2 d_3 - \alpha_3 d_6 - \beta_3 d_5$

(ii) Couple stress coefficient:

The non – dimensional Couples Stress at the plate $y = 0$ due to rotational motion is given as:

$$M_w = \left(\frac{\partial N}{\partial y} \right)_{y=0} = (-\alpha_1 b_1 + b_2 \beta_1) \cos \omega t + (b_1 \beta_1 + \alpha_1 b_2) \sin \omega t$$

The Couple stress coefficient is obtained as:

$$C_m = \frac{\nu M_w}{V_0^3} = 2(1+ j(1-n)) \left(\frac{\partial u}{\partial y} \right)_{y=0}$$

Further calculation gives,

$$C_m = .\left(1+\frac{1}{2} j\right) N'(0) = .\left(1+\frac{1}{2} j\right)\left[\left(-b_1\alpha_1 + b_2\beta_1\right) \cos \omega t + \left(b_2\alpha_1 + b_1\beta_1\right) \sin \omega t \right]$$

(iii) Nusselt number:

The non – dimensional heat transfer rate at the plate $y = 0$ is given as:

$$Nu_R = -\frac{1}{\Pr} \left(\frac{\partial \theta_R}{\partial y} \right)_{y=0} = \frac{A}{\Pr} \left[-\alpha_2 \cos \omega t + \beta_2 \sin \omega t \right]$$

(iv) Sherwood number:

The non – dimensional mass transfer rate at the plate $y = 0$ is given as:

$$Sh_R = -\frac{1}{Sc} \left(\frac{\partial \phi_r}{\partial y} \right)_{y=0} = \frac{1}{Sc} \left(-\alpha_3 \cos \omega t + \beta_3 \sin \omega t \right)$$

5. RESULTS AND DISCUSSION

For numerical simulation of the results, the values of the governing parameters are taken along with the graphs. In this study Prandtl number (*Pr*) is taken as0.71 at 298K.

The physical effect of the pertinent parameters such as Prandtl number (*Pr*), amplitude correction parameter (*A*) on the non-dimensional temperature profiles (θ_R, y) are shown graphically in figures 2 and 3 respectively. It is observed that, the fluid temperature is being decreased due to increase in values of *Pr*, while a reversed phenomenon has observed in presence of *A*. The increase in values of *Pr* decreases the thickness of the thermal boundary layer, which results in decrease the temperature near the plate surface. On the other hand, due to positive increase in values of *A*, increases the amplitude of oscillation of the temperature wave within the thermal boundary layer, thereby increases the temperature near the plate surface. The figure 4 expresses the influence of Schmidt number (*Sc*) on the non-dimensional concentration profiles (ϕ_R, y). Due to increase in Schmidt number, the Brownian mass diffusion coefficient decreases as such, the temperature within the thermal boundary layer diminishes.

The parametric influences of various field parameters like microrotation proportional parameter (*n*), vortex viscosity parameter *(j)* and dimensionless material parameter (*s*) on the linear fluid velocity u_R as well as on the rotational fluid velocity N_R have been demonstrated graphically in figures 5 to 10 respectively. The increase in values of *n* results in a fluctuation effect on the linear flow rate but found diminishing the rotational flow rate. It is observed that, the linear flow rate increases immensely near to the plate region approximately for $y \in [0, 1.25]$, which is supposed to be strongly concentrated micropolar fluid region, while far away from the plate for $y \in [1.25, 3.50]$ (approximately),

considered to be a weekly concentrated micropolar fluid domain, the flow shows a narrow decreasing trend. Again as y increases approximately for y > 3.5, the flow becomes steady. On the other hand as *n* increases, the microrotation becomes continuously in decreasing trend, which diminishes far away from the plate and attains a steady state approximately for y ≥ 1.7. For $j \neq 0$, the linear momentum equation (7) becomes uncoupled from the angular momentum equation (8). It is interesting to observe that, the linear velocity attains a peak, where the inclination of the linear velocity slopes with the positive normal direction increases significantly with decreasing j near to the wall

surface approximately for $y \in [0, 0.65]$ and for $y \in (0.65, 2.5]$, the peak diminishes with an increasing velocity slopes as *j* increases. Again for y > 2.5, the velocity slope achieves a slight increasing trend and tries to attend a steady state. On the other hand, as *j* increases, the couple stresses increase near the plate region due to high concentration of micropolar fluid, there by diminishes the rotational effect of fluid up to $y \approx 1.5$, which is characterized by a continuous increase of the micropolar velocity slopes with the normal scale. Again, for $y > 1.5$ a steady state is observed. Due to increase in dimensionless material parameter *s*, the microrotation diffusivity decreases. This increases the linear momentum diffusivity and as such the flow rate increases and is found to increase the linear velocity approximately for $y \in [0, 0.70]$. When, $y \in (0.70, 2.0]$, the linear velocity slope increases with increase in values of *s*, which causes the linear velocity to increase in that region and for $y > 2.0$, no significant differences observed and the linear velocity trend is found to attain a steady state while, the microrotation is found to decrease for $y \in [0, 2.0]$ due to the obvious reason and a steady microrotation state has observed for y > 2.0. On the other hand, the microrotation flow rate is found to decelerate due to increase in values of *s* within the flow region for normal distances $y \in [0, 1.9]$. This is obvious as microrotation diffusivity decreases due to increase in parametric values of *s*.

Figures 11 to 14 depict the influence of parameters like *Gr* and *Gm* on the linear velocity u_R as well as on the microrotational fluid velocity N_R against normal distances *y* respectively. The increase in values of *Gr* and *Gm* respectively increases the thermal buoyancy as well as mass buoyancy forces while producing a resistive effect by generating extra stress to rotational motion. The effect of Prandtl number *Pr* on the Nusselt number *Nu* against time *t* is shown in figure 15. The increase in Prandtl number decreases the thermal diffusivity as such the heat fluxes get transmitted along the cross – radial direction, which thus increase the value of Nusselt number. In figure 16 the parametric intervention of Schmidt number upon Sherwood number is demonstrated. The rise in Schmidt number decreases the Brownian mass diffusivity, results of which a cross directional mass transmission takes place, which is seen to increase the Sherwood number. The figures 17 and 18 exhibit the outcome of the presence of vortex viscosity parameter (*j*) on the skin- friction co-efficient as well as on the couple stress co-efficient respectively. Due to increase in values of *j*, the resistive forces increase, this increase the skin-friction as well as the couple stress co-efficient. The influence of microrotation proportionality parameter (*n*) on the skin- friction co-efficient as well as on the couple stress co-efficient is demonstrated in figures 19 and 20 respectively. It is observed that, for $t \in [0.0.2]$ (approximately), both the skin-friction co-efficient and the couple stress co-efficient are found increasing due to increase in values of *n*. In table 1, a numerical variation of the values of the skin-friction co-efficient against a set of parametric values of thermal Grashof number (*Gr*), solutal Grashof number (*Gm*) and permeability parameter (*K*) is highlighted to display a comparison between micropolar fluid flows with that of the Newtonian fluid case. It is clearly observed from the table that, the skin – friction co - efficient in both the cases increases due to increase in *Gr* as well as *Gm*, while in both the cases the skin – friction co - efficient found decreasing for an increase in values of *K*. It is also interesting to observe that, the frictional effect in micropolar fluid case is less than that of the Newtonian case showing thereby the importance of the theory of micropolar fluid flow.

6. CONCLUSIONS

A theoretical study has been conducted to investigate the physical effects of proportional parameter, dimensionless material parameter and vortex viscosity parameter on the laminar two-dimensional flow of micropolar fluid flow. The investigation reveals that, the linear velocity increases as the microrotation proportional parameter, dimensionless material parameter as well as the thermal and solutal Grashof numbers increase, while the angular velocity of the fluid particles shows just an opposite results for the parametric increase of the said non-dimensional parameters. Again as expected an increase in values of vortex viscosity parameter increases the angular velocity but decreases the linear velocity of the fluid particles. Due to increase in vortex viscosity parameter *j* and for $t \in [0.0.2]$ (approximately), the skin –friction co –efficient as well as the couple stress co –efficient are found to be in increasing trend. The increase in Prandtl number and microrotation proportional parameter *n* increases the skin-friction co-efficient, while couple stress co-efficient increases due to increase in proportional parameter but found decreasing due to Prandtl number. Finally, the plate friction is found to be more in Newtonian fluid than in micropolar fluid. Thus it is possible to control the surface friction by applying the theory of micropolar fluids.

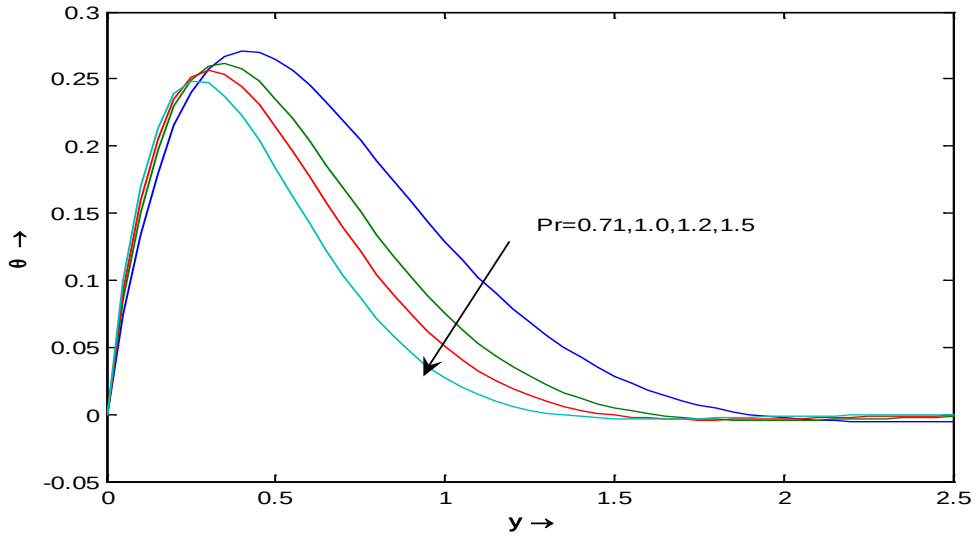

Figure-2: Graph of temperature θ versus normal distance *y* for fixed values of *A=1.0*, ω =7.857143, *t*=0.

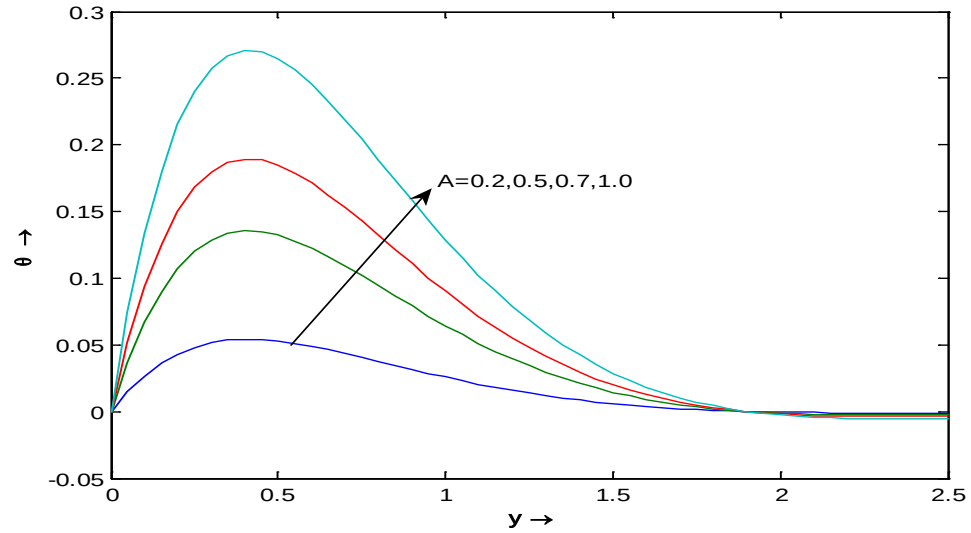

Figure-3: Graph of temperature θ versus normal distance y for fixed values of *Pr=0.71*, ω =7.857143, t=0.2

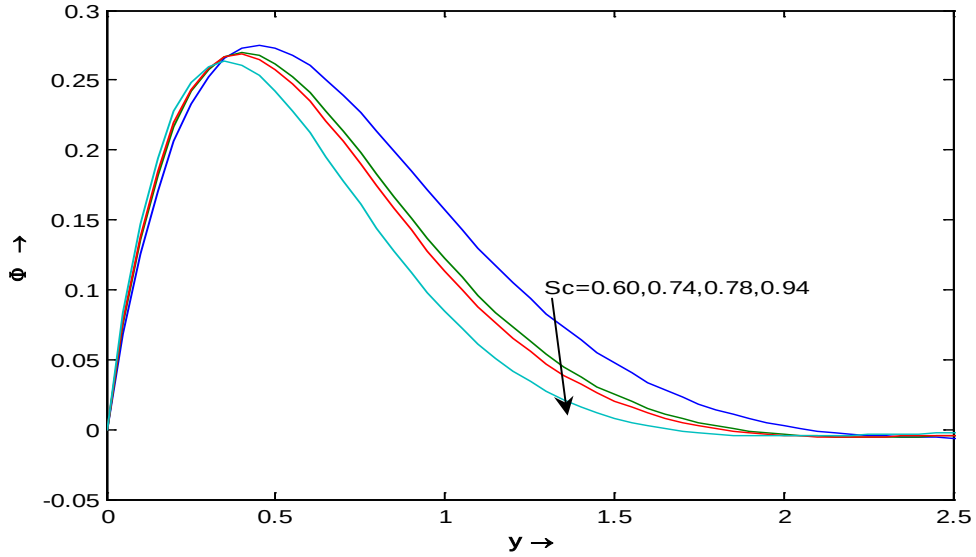

Figure-4: Graph of concentration ϕ versus normal distance y for fixed values of ω =7.857143, t= 0.2

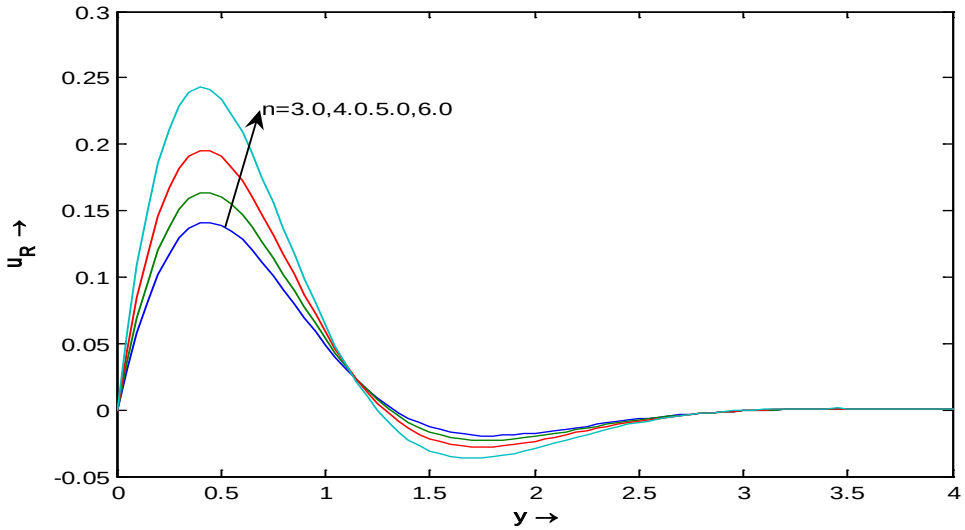

Figure-5: Graph of velocity u_R versus normal distance y for fixed values of *A*=1.0, *k*=0.5, *s*=0.8, j=0.5, *Gr*=2.0, *Gm*=1.0, ω =7.857143, ωt =1.57143

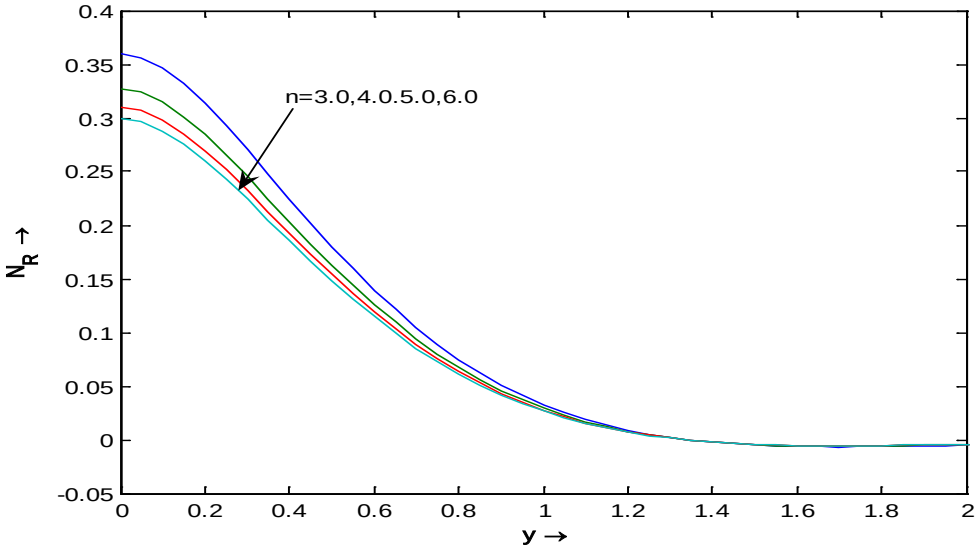

Figure- 6: Graph of angular momentum N_R versus normal distance y for fixed values of *A*=1.0, *k*=0.5, *s*=0.8, *j*=0.5, *Gr*=2.0, *Gm*=1.0, ω =7.857143, ωt =1.57143

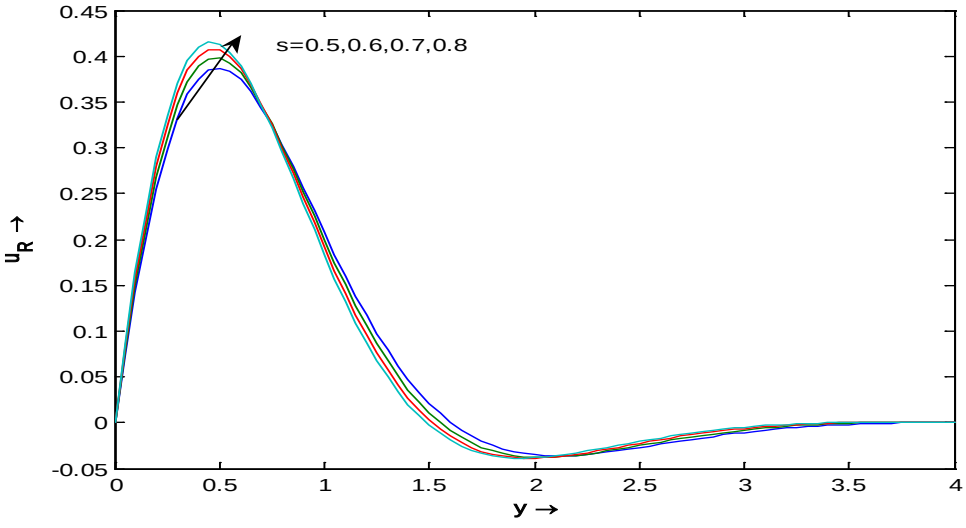

Figure-7: Graph of velocity versus normal distance y for fixed values of *A*=3.0, *Pr*=0.71, *Sc*=0.60, *n*=3.0, *k*=0.5, *Gr*=2.0, *Gm*=1.0

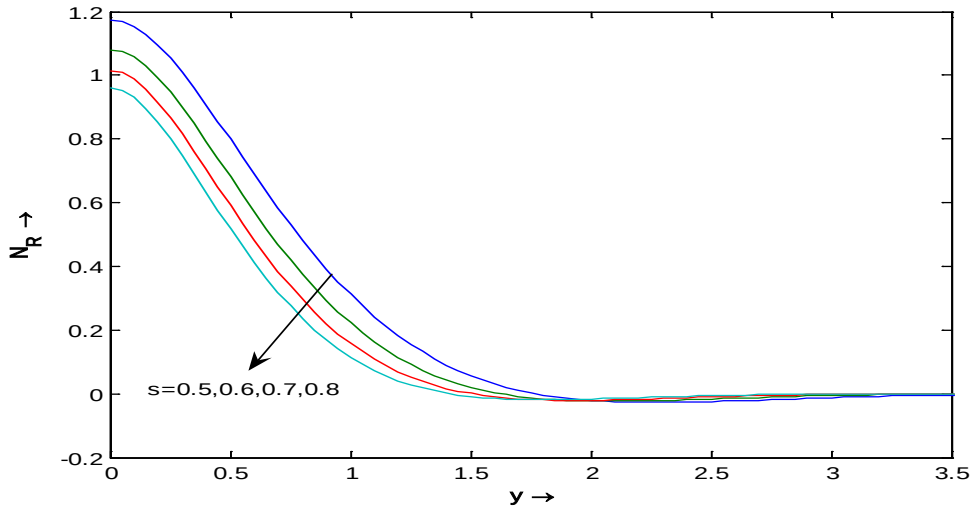

Figure-8: Graph of angular momentum N_R versus normal distance *y* for fixed values of *A*=3.0,*Pr*=0.71, *k*=0.5, *Sc*=0.60, *n*=3.0, *Gr*=2.0,*Gm*=1.0.

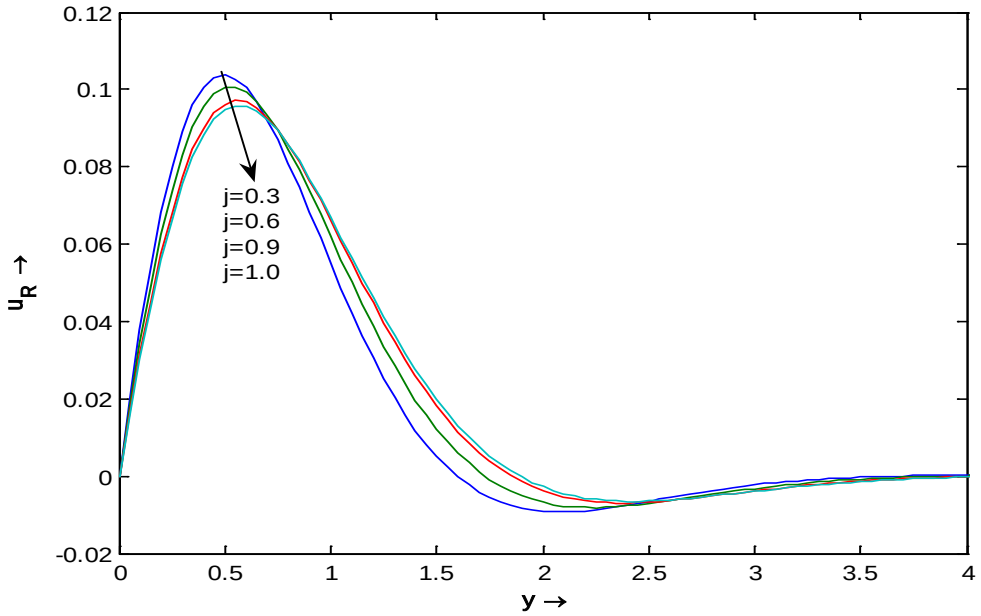

Figure-9: Graph of velocity versus normal distance for variation of vortex viscosity parameter for fixed values of *A*=0.01, *Pr*=0.71, *s*=0.5, *Gr*=1.0, Gm=0.5, *Sc*=0.60, *n*=0.5, *k*=0.5, *s*=0.8

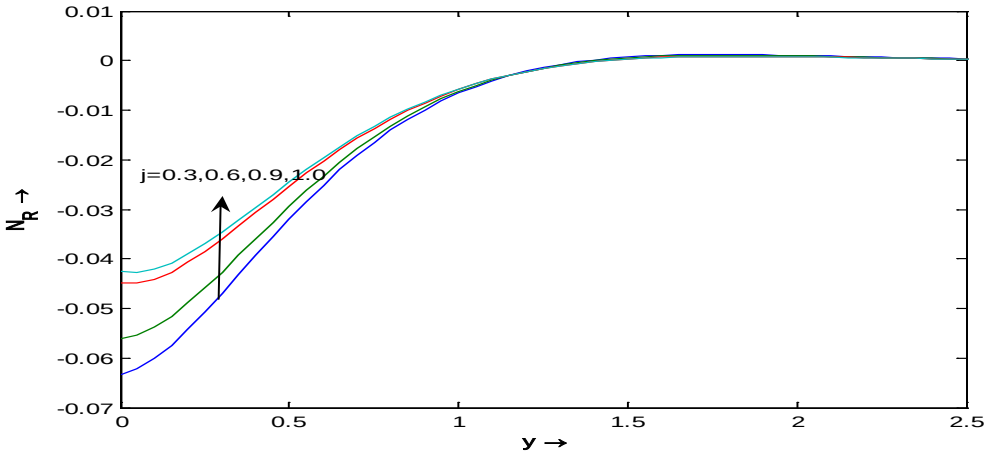

Figure-10: Graph of angular momentum N_R versus normal distance *y* for fixed values of *A*=0.01, *Pr*=0.71, *s*=0.8, *Gr*=1.0, *Gm*=0.5, *n*=0.5, *k*=0.5,

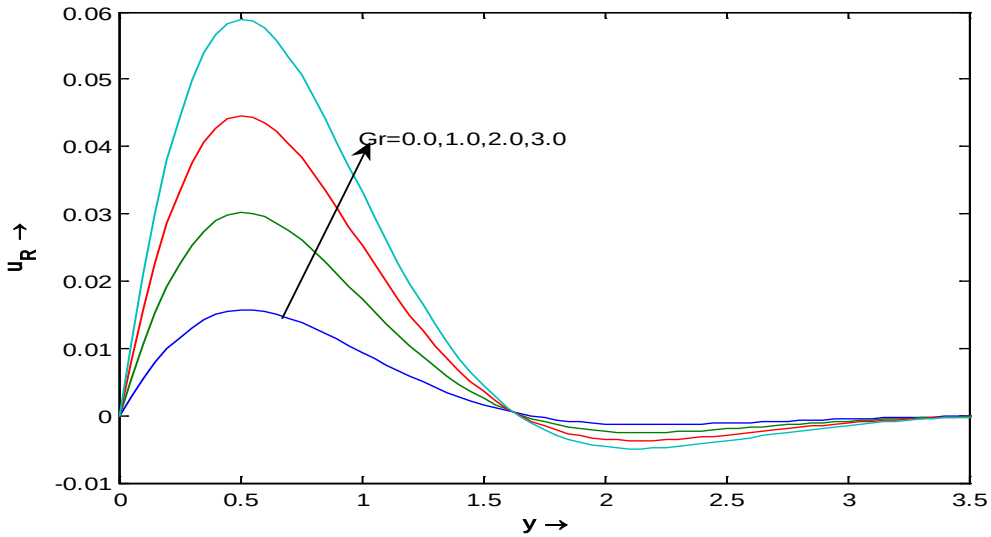

Figure-11: Graph of linear velocity u_R versus normal distance *y* for fixed values of *A*=0.5, ω =7.857143, ωt =1.57143, *n*=0.5, *Sc*=0.60, *j*=0.5, *Gm*=0.5

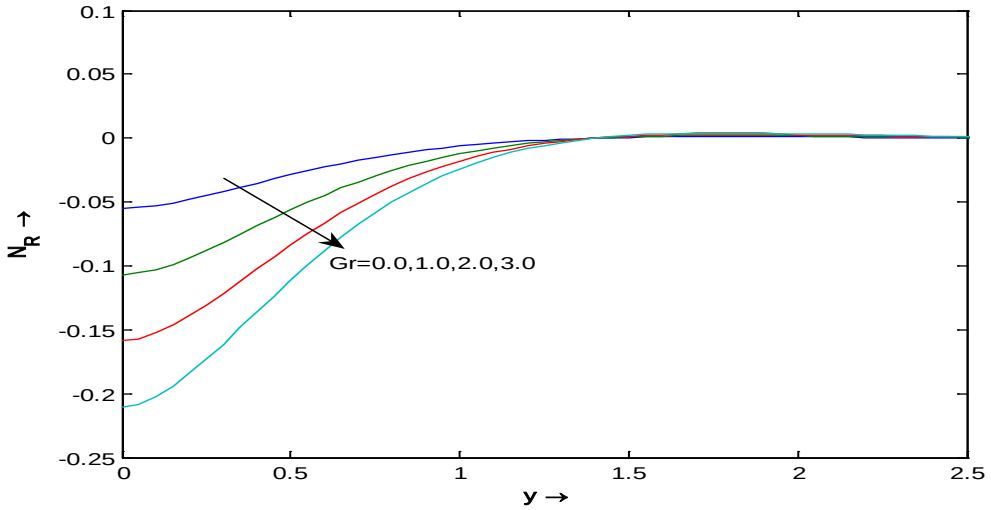

Figure-12: Graph of angular momentum N_R versus normal distance y for fixed values of *A*=0.5, ω =7.857143, ωt =1.57143, *n*=0.5, *Sc*=0.60, *j*=0.5, *Gm*=0.5, *s*=0.5, *k*=0.5

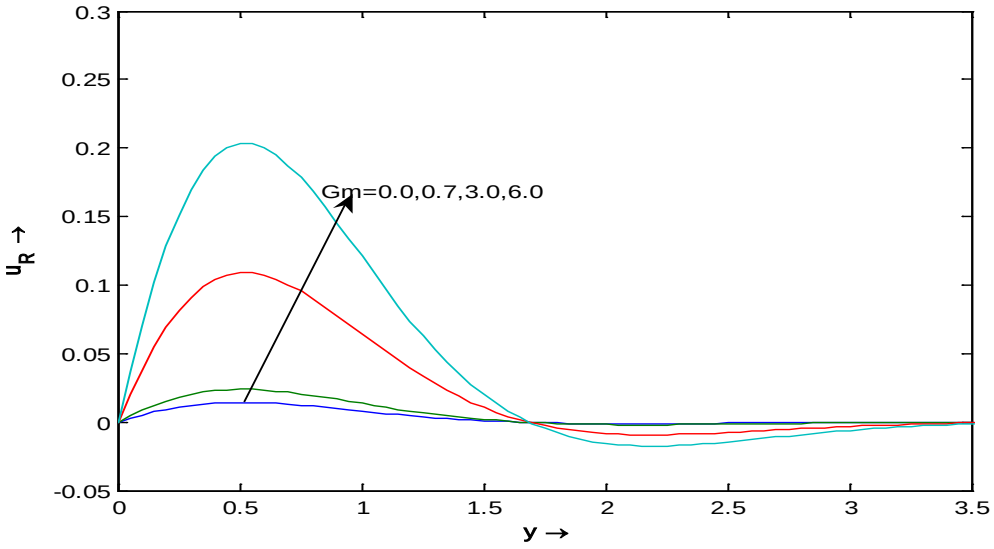

Figure-13: Graph of linear velocity u_R versus normal distance *y* for fixed values of *A*=0.5, ω =7.857143, ωt =1.57143, *Pr*=0.71, *Sc*=0.60, $Gr = 1.0$, *j*=0.5,*k*=0.5, *s*=0.8

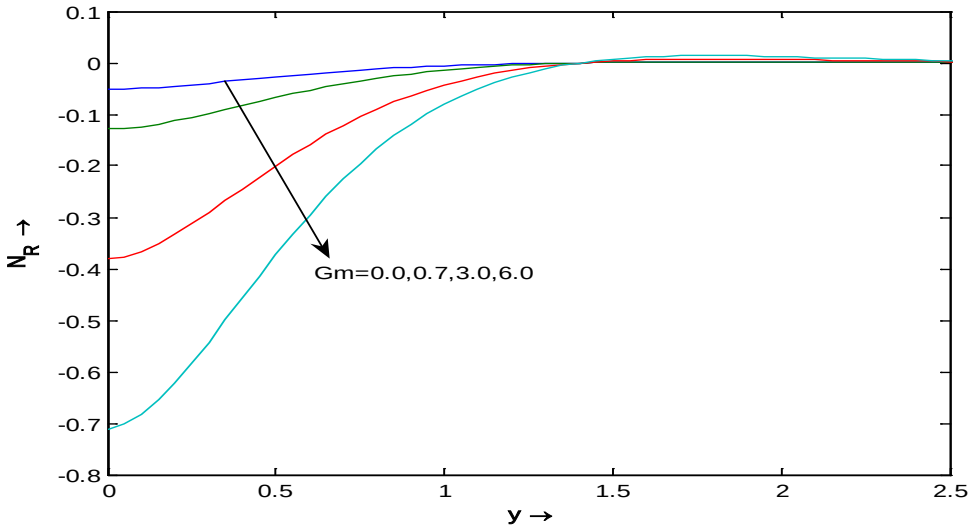

Figure-14: Graph of angular momentum N_R versus normal distance y for fixed values of *A*=0.5, ω =7.857143, ωt =1.57143, *Pr*=0.71, *Sc*=0.60, $Gr = 1.0$, *j*=0.5, *s*=0.5, *k*=0.5

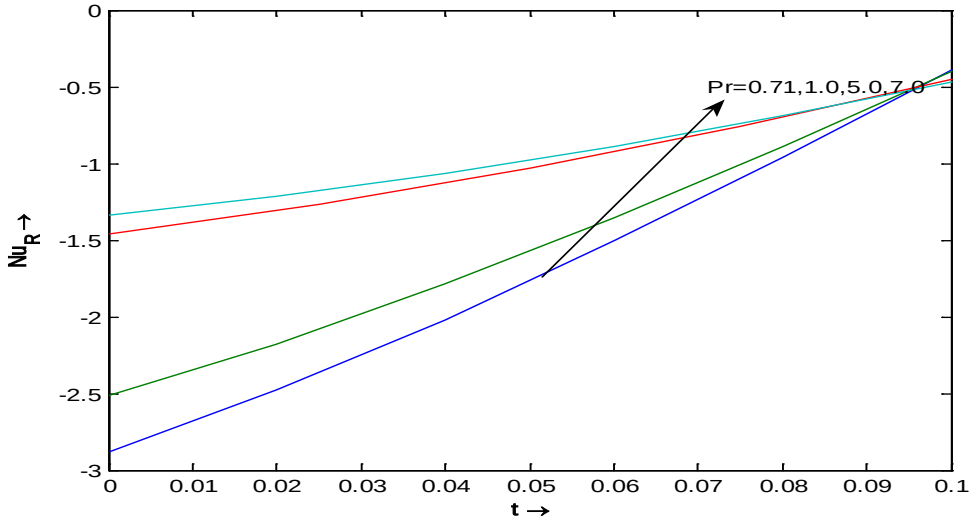

Figure-15: Graph of Nusselt number(Nu_R) versus time *t* for fixed values of *Pr*=0.71, ω =7.857143, *t*=0.2

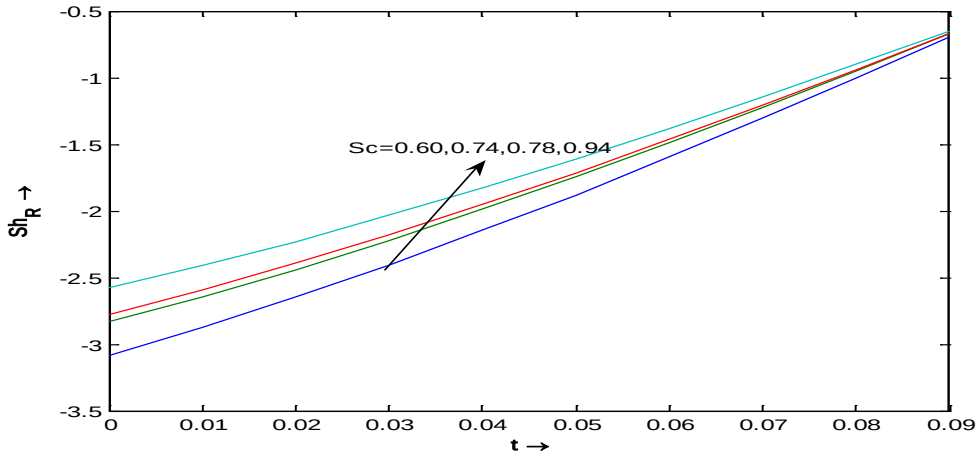

Figure-16: Graph of Sherwood number Sh_R versus time t for fixed values of ω =7.857143, *t*=0.2

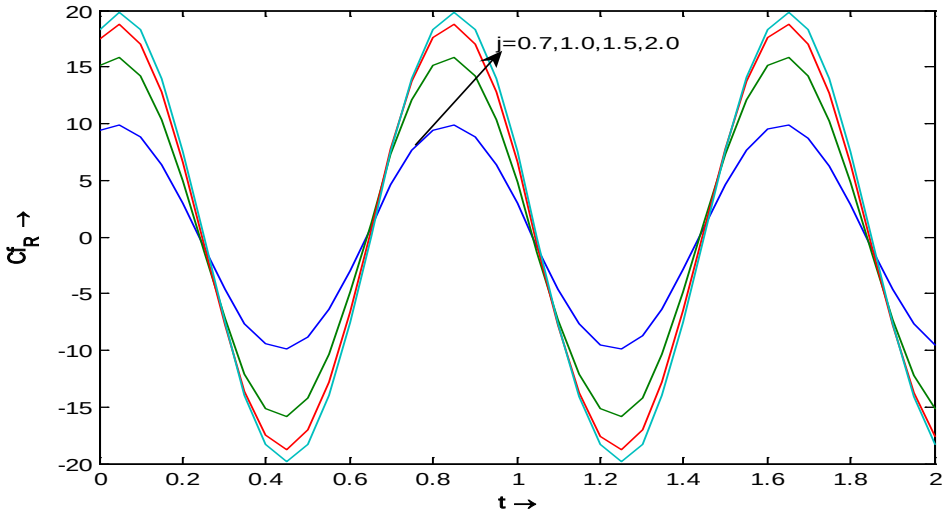

Figure -17: Graph of skin friction coefficient (Cf_R) versus time t for A=3.0, Pr=0.71, Sc=0.60, ω =7.857143, t=0.2, n=3.0, s=3.0, Gr=3.0, Gm=1.0, k=1.0

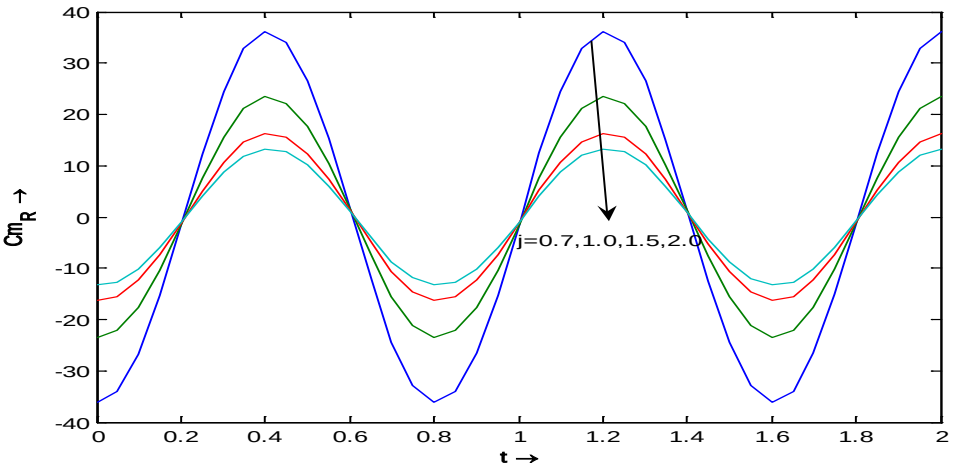

Figure-18: Graph of Couple stress coefficient (Cm_R) versus time t for fixed values of A=3.0, Pr=0.71, Sc=0.60, ω =7.857143, t=0.2, n=3.0, s=3.0, Gr=3.0, Gm=1.0, k=1.0

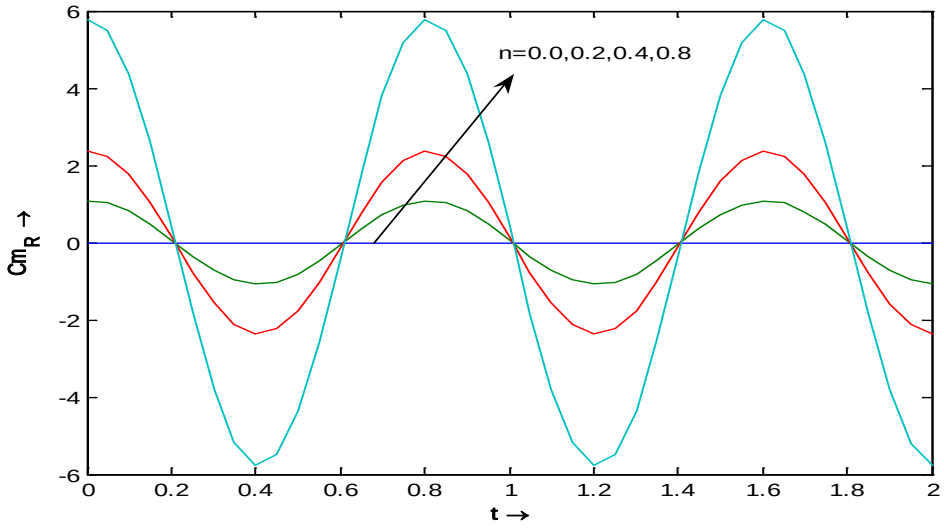

Figure -19: Graph of Couple stress coefficient (Cm_R) versus time t for fixed values of A=3.0, Pr=0.71, Sc=0.60, ω =7.857143, t=0.2, n=3.0, s=3.0, Gr=3.0, Gm=1.0, k=1.0

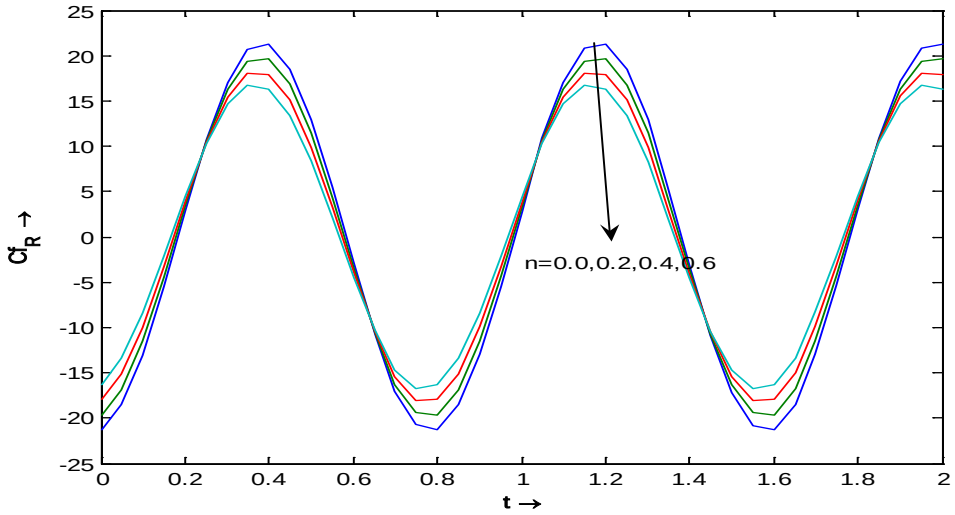

Figure-20: Graph of skin friction coefficient (Cf_R) versus time t for A=3.0, Pr=0.71, Sc=0.60, ω =7.857143, t=0.2, j=0.5, s=0.8, Gr=3.0, Gm=1.0, k=1.0

Table-1: Table showing a comparison between micropolar fluid and Newtonian fluid cases for skin – frction co-efficients:

C_f	*Gr*				*Gm*				*K*			
	1.5	2.0	2.5	3.0	1.0	1.5	1.7	2.0	0.6	0.7	0.8	0.9
For Micro polar fluid	0.0250	0.0173	0.0095	0.0017	0.0017	0.0259	0.0356	0.0501	0.0456	0.0345	0.0236	0.0127
For Newtonian Fluid	0.0277	0.0342	0.0406	0.0470	0.0470	0.0512	0.0529	0.0555	0.0494	0.0485	0.0478	0.0473

APPENDIX

$$\alpha_1 = \frac{1}{2}\left[s + \sqrt{\frac{s}{2}}\left(s + \sqrt{s^2 + 16w^2}\right)^{1/2}\right],\ \beta_1 = \frac{1}{2}\left[\sqrt{\frac{s}{2}}\left(s + \sqrt{s^2 + 16w^2}\right)^{1/2}\right]$$

$$\alpha_2 = \frac{1}{2}\left[P_r + \sqrt{\frac{P_r}{2}}\left(P_r + \sqrt{P_r^2 + 16w^2}\right)^{1/2}\right]\ \beta_2 = \frac{1}{2}\left[\sqrt{\frac{P_r}{2}}\left(P_r + \sqrt{P_r^2 + 16w^2}\right)^{1/2}\right]$$

$$\alpha_3 = \frac{1}{2}\left[S_c + \sqrt{\frac{S}{2}}\left(S_c + \sqrt{S_c^2 + 16w^2}\right)^{1/2}\right]\ \beta_3 = \frac{1}{2}\left[\sqrt{\frac{S_c}{2}}\left(S_c + \sqrt{Sc^2 + 16w^2}\right)^{1/2}\right]$$

$$r_1 = \sqrt{\left(1 + 4M_1 j_1\right)^2 + 16\omega^2 j_1^2}\ ,\ M_1 = \frac{1+j}{k}\ ,\ j_1 = 1 + j\ ,\ \alpha_4 = \frac{1 + \frac{1}{\sqrt{2}}\left[-\left(1 + 4M_1 j_1\right) + r_1\right]^{\frac{1}{2}}}{2 j_1}$$

$$\beta_4 = \frac{\left[-\left(1 + 4M_1 j_1\right) + r_1\right]^{\frac{1}{2}}}{2\sqrt{2}\, j_1},\ a_1 = j_1\alpha_1^{\,2} - \alpha_1 - M_1 - j_1\beta_1^{\,2},\ a_2 = 2 j_1\alpha_2\beta_2 - \beta_2 - \omega,$$

$$d_1 = \frac{\left(a_1\alpha_1 + a_2\beta_1\right)2 j_1}{a_1^2 + a_2^2},\ d_2 = \frac{\left(a_1\beta_1 - a_2\alpha_1\right)2 j_1}{a_1^2 + a_2^2},\ a_3 = j_1\alpha_2^{\,2} - \alpha_2 - M_1 - j_1\beta_2^{\,2},$$

$$a_4 = 2 j_1\alpha_2\beta_2 - \beta_2 - \omega$$

$$d_3 = \frac{-GrAa_3}{a_3^2 + a_4^2},\ d_4 = \frac{GrAa_4}{a_3^2 + a_4^2},\ a_5 = j_1\alpha_3^{\,2} - \alpha_3 - M_1 - j_1\beta_3^{\,2},\ a_6 = 2 j_1\alpha_3\beta_3 - \beta_3 - \omega$$

$$d_5 = \frac{-Gm \cdot a_5}{a_5^2 + a_6^2}, d_6 = \frac{Gma_6}{a_5^2 + a_6^2}\ , A_1 = 1 + n\alpha_4 d_1 - n\beta_4 d_2 - n\alpha_1 d_1 + n\beta_1 d_2\ ,$$

$$A_2 = -n\alpha_4 d_2 - n\beta_4 d_1 + n\alpha_1 d_2 + n\beta_1 d_1$$

$$c_1 = n\left[\alpha_4\left(d_3+d_5\right)-\beta_4\left(d_4+d_6\right)-\alpha_2 d_3+d_4\beta_2-\alpha_3 d_5+\beta_3 d_6\right]$$

$$c_2 = n\left[\alpha_4\left(d_4+d_6\right)+\beta_4\left(d_3+d_5\right)-\alpha_2 d_4-d_3\beta_2-\alpha_3 d_6-\beta_3 d_5\right]$$

$$b_1 = \frac{A_2c_2-A_1c_1}{A_1^2+A_2^2}, b_2 = \frac{-A_2c_1-A_1c_2}{A_1^2+A_2^2}, e_1 = -b_1d_1+b_2d_2-d_3-d_5, e_2 = -b_2d_1-b_1d_2-d_4-d_6$$

7. REFERENCES

1. Alam M. S, Hossain S. M. C., A new similarity approach for an unsteady two-dimensional forced convective flow of a micropolar fluid along a wedge, J. Appl. Math. Mech. 9 (2013), 75-89.
2. Ali J. C., Ali Al-Mudhaf, Jasem Al-Yatama, Double diffusive convective flow of a micropolar fluid over a vertical plate embedded in a porous medium with chemical reaction, Inter. J. Fluid Mech. Res. 31(6) (2004), 529–551.
3. Ariman T., Turk M.A., Sylvester N.D. Microcontinuum fluid mechanics. A review, Inter. J.Fluid. Mech.11 (1973), 905-930.
4. Ariman T., Turk M.A., Sylvester N.D. Applications of microcontinuum fluid mechanics, A review, Int. J.Eng.Sci. 12(1974), 273-293.
5. Ahmad F., Hussain S., Convective heat transfer for MHD micropolar fluids flow through porous medium over a stretching surface, JAEBS, 5(2015), 6-12.
6. Bakr A.A., Effects of chemical reaction on MHD free convection and mass transfer flow of a micropolar fluid with oscillatory plate velocity and constant heat source in a rotating frame of reference, Commun. Nonlinear Sci. Numerical Simul. 16(2011), 698–710.
7. Bejan A., Khair K.R., Heat and mass transfer by natural convection in a porous medium, Int. J. HeatMass Transf. 28(1985), 909 - 918.
8. Chaudhary D., Singh H., Jain N.C., Unsteady magnetopolar free convection flow embedded in a porous medium with radiation and variable suction in a slip flow regime, IJMSI, 1(1) (2013), 01-11.
9. Cortell R., Flow and heat transfer of a fluid through a porous medium over a stretchingsurface with internal heat generation/absorption and suction/blowing, Fluid. Dyn. Res. 37(4), (2005), 231.
10. Damseh R.A., Azab T.A.A., Shannak B.A., Husein M.A., Unsteady natural convection heat transfer of micropolar fluid over a vertical surface with constant heat flux. Turkish J. Eng. Env. Sci. 31(2007), 225-233.
11. Das K., Effect of chemical reaction and thermal radiation on heat and mass transfer flow of MHD micropolar fluid in a rotating frame of reference, Int. J. Heat Mass Transf. 54 (2011), 3505–3513.
12. Eringen A.C., Theory of thermomicropolar fluids, J. of Mathematics and Mechanics, 16(1966), 1–18.
13. Eringen A. C., Theory of thermomicropolar fluids, J. Math. Anal. Appl. 38(1972), 480-496.
14. Haque Md.Z., Alam Md. M., Ferdowsb M., Postelnicu A., Micropolar fluid behaviors on steady MHD free convection and mass transfer flow with constant heat and mass fluxes, joule heating and viscous dissipation, JKSUES, 24(2012), 71–84.
15. Javaherdeh K., Nejad M.M., Moslemi M., Natural convection heat and mass transfer in MHD fluid flow past a moving vertical plate with variable surface temperature and concentration in a porous medium, JESTECH,18(2015), 423-431.
16. Kim Y. J., Heat and Mass Transfer in MHD micropolar flow over a vertical moving porous plate in a porous medium, TPM, 56(2004), 17–37.
17. Kim Y.J., Unsteady convection flow of micropolar fluids past a vertical porousmedium, Acta. Mech. 148(2001), 106–116.
18. Makinde O.D., Free convection flow with thermal radiation and mass transfer past a moving vertical porous plate, Int. J. Heat Mass Transf.25 (2005), 289-295.
19. Mohammad M.R., Muhammad A., Behnam R., Mohammad T.R., Sumra B., Mixed convection boundary-layer flow of a micropolar fluid towards a heated shrinking sheet by homotopy analysis method, Therm. Sci. 20(1) (2016), 21-34.
20. Oahimire J. I., Olajuwon B. I., Effects of radiation absorption and thermo-diffusion on MHD heat and mass transfer flow of a micro-polar fluid in the presence of heat Source, Appl. Appl. Math. 9(2014), 763-779.
21. Ojjela O., Naresh K. N., Unsteady MHD mixed convection flow of chemically reacting micropolar fluid between porous parallel plates with Soret and Dufour effects, Journal of Engineering. (2016), Article ID 6531948, 13 pages.
22. Prathap K. J., Umavathi J. C., Ali J. Chamkha, Ioan pop fully-developed free-convective flow of micropolar and viscous fluids in a vertical channel, Appl. Math. Model. 34(2010), 1175–1186.
23. Raptis A., Unsteady free convection flow through a porous medium, Int. J.Eng.Sci. 21(4) (1983), 345-349.
24. Rashidi M.M., Rostami B., Freidoonimehr N., Abbasbandy S., Free convective heat and mass transfer for MHD fluid flow over a permeable vertical stretching sheet in the presence of the radiation and buoyancy effects, Ain Shams Eng. J. 5(3) (2014), 901–912.

25. Rawat S., Bhargava R., Renu Bhargava R., Anwar Bég O., Transient Magneto-Micropolar free convection heat and mass transfer through a non-darcy Porous medium channel with variable thermal conductivity and heat source effects, Journal of Mechanical Engineering Science. 223(2009), 2341–2355.
26. Seddek M.A., Odda S.N., Akl M.Y., Abdelmeguid M.S., Analytical solution for the effect of radiation on flow of a magneto-micropolar fluid past a continuously moving plate with suction and blowing, Comput. Mater. Sci.45(2009), 423–428.
27. Soundalgekar V. M., Free convection effects on the oscillatory flow past an infinite, vertical, porous plate with constant suction, Proc. R. Soc. A. 333(1973), 25– 36.
28. Yucel A., Mixed convection micropolar fluid flow over horizontal plate with surface mass transfer, Int. J. Eng. Sci. 27(1989), 1593–1608.

Source of support: Nil, Conflict of interest: None Declared.